GL03978

Geothermics (1970) - SPECIAL ISSUE 2

U. N. Symposium on the Development and Utilization of Geothermal Resources, Pisa 1970. Vol. 2, Part 2

Some Geothermal Measurements at the Otake Geothermal Area

M. FUKUDA *, K. USHIJMA *, K. AOSAKI ** AND N. YAMAMURO **

ABSTRACT

For the purpose of preparing the fundamental data on the problems of geothermal development, thermal discharge, temperature gradient and thermal conductivity of rock samples were measured at Otake geothermal area.

In a geothermal area, generally, heat is discharged by various processes, such as fumaroles, which can be classified under several headings according to their discharge amount, hot springs and hot ground surfaces. The heat flow from the strong fumaroles was measured by condensing the natural steam in the water vessel and the heat flow from the weak ones was measured by using a wet and dry bulb thermometer.

Several holes were drilled in the thermal area to determine the underground temperature gradient which is 1.9 °C/m at the steaming ground and 0.8 °C/m at the ordinary geothermal area.

The thermal conductivity of 30 dried core samples was measured in the laboratory and in situ by means of the line source method. The range is $7.73 \times 10^{-4} \sim 1.72 \times 10^{-2}$ cal/sec cm °C and it was noted that the thermal conductivity of unaltered rocks is greater than that of altered ones.

Introduction

The Otake geothermal area is located 900-1000 m above sea level and forms a basin-like topography surrounded by volcanic domes. The river Kusu flows to the north through the central part of the area. The Kawara, Otake, Komatsu fumaroles and some hot springs lie on the right side of the river (Figures 1, 7, 8 and 9).

From the results of geological surveys, geophysical explorations, test bores and so on, it was confirmed that the geothermal area was elliptical in plan, about 3 km long from north to south, by about 1 km wide from east to west.

In order to prepare the fundamental data on the problems of geothermal development, the thermal discharge, temperature gradient and thermal conductivity of rock samples were measured at the Otake geothermal area.

Measurement of thermal discharge

The thermal discharge from a geothermal area may be classified as follows from the viewpoint of discharging processes:

a - steam
b - hot springs
c - heat transfer at the ground surface
d - gas.

In the process of computing the quantity of thermal discharge, the mean annual temperature in a normal area has to be used as a basic temperature. However, in an engineering field, the enthalpy at temperature of 0 °C is frequently used, so we applied 0 °C.

THERMAL DISCHARGE BY STEAM

The condensing method was used for the heat loss from strong fumaroles and the calorimeter method was used for weak ones. These methods are described briefly as follows.

Condensing method. The condenser is shown in Figure 2. This instrument is essentially a device for measuring the temperature and amount of condensed water discharged from a sample area of the steaming ground. Placing a cone vessel over the vent, natural steam from a fumarole was fed into a water bath and the thermal discharge by steam can be computed by the following equation of the form:

$$Q = [dG\,(t+dt) + G \cdot dt] \,/\, A$$

where

Q is the thermal discharge by steam, dG the amount of condensed water, t the initial temperature of the water bath, dt the value of temperature rise, G the amount of water in a water bath initially and A is the area of the bottom of the vessel.

A fan was used in the practical measurement so that the flow of steam might be unaffected by the presence of the vessel. The inner pressure of the vessels was checked with a manometer.

Calorimeter method. The calorimeter is shown in Figure 3. It is essentially a box having an open bottom of 1 m². Both the wet-bulb and dry-bulb temperatures at inlet and outlet were measured. The air speed was measured by the anemometer set at the ports. From these measurements, the heat flow can be calculated by the following equation:

$$Q = M\,(i_2 - i_1) \,/\, A$$

where

Q is the amount of thermal discharge, M the amount of air, i the enthalpy (subscript 1 and 2 correspond to inlet and outlet of the calorimeter, respectively), A is the area of the bottom of the vessel.

For the computation of the heat flow, the moist-air diagram made by H. UCHIDA was used. The calorimeter

* Research Institute of Industrial Science, Kyushu University, Faculty of Mining Engineering, Kyushu, Japan.
** Kyushu Electric Power Co., Ltd, Kyushu, Japan.

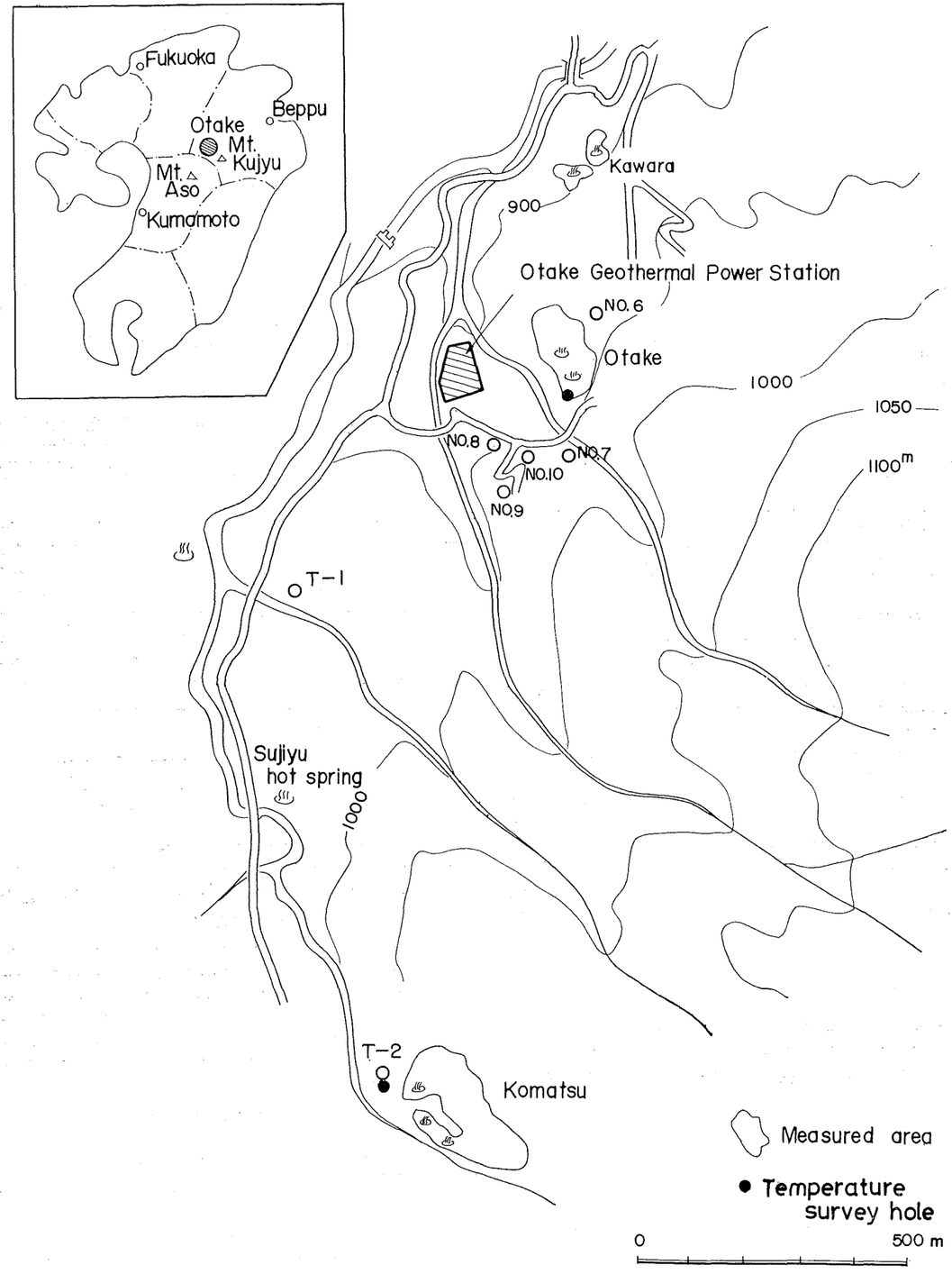

FIG. 1. — *Otake geothermal area.* T-1, T-2: *test wells;* No. 6, No. 7, No. 8, No. 9, No. 10: *productive wells.*

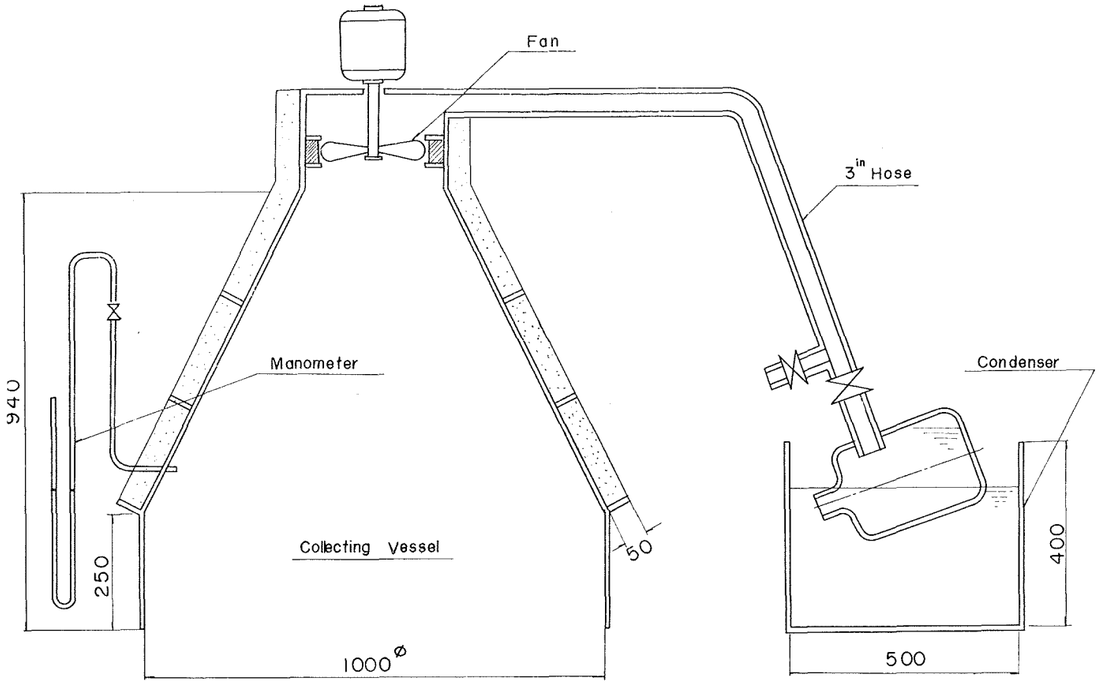

FIG. 2. — *Condenser.*

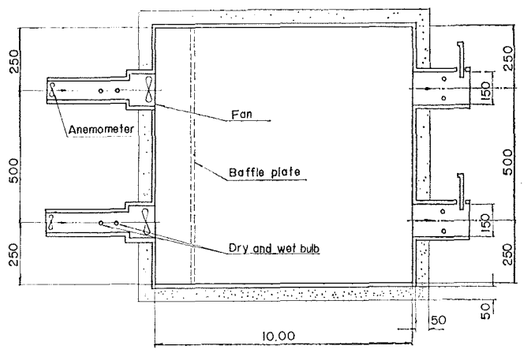

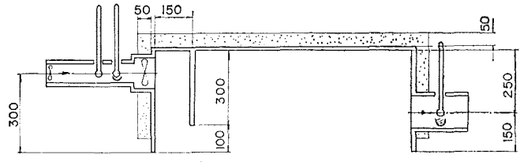

FIG. 3. — *Calorimeter.*

was calibrated in the laboratory. The calibration curve is shown in Figure 4.

THERMAL DISCHARGE BY HOT SPRINGS

The volume of water flow was measured with either a weir or a float, according to the geographical position. The thermal discharge by hot springs is computed by the equation:

$$Q = \rho \cdot c \cdot V\,(t_2 - t_1)$$

where

Q is the amount of heat discharge by hot water, ρ the density of the water, c the specific heat of the water, V the flow rate of the water, t_2 the temperature of hot springs and t_1 is the basic temperature.

THERMAL DISCHARGE BY HEAT TRANSFER AT THE GROUND SURFACE.

A relation between the temperature at the depth of 5 cm and the thermal discharge, measured by the calorimeter, was obtained as shown in Figure 5. From this relation and the temperature at the depth of 5 cm measured in meshes of a net of 20 m span, the thermal discharge was determined. The area in which the thermal discharge was more than 10 kcal/m² h was adopted here as the geothermal area.

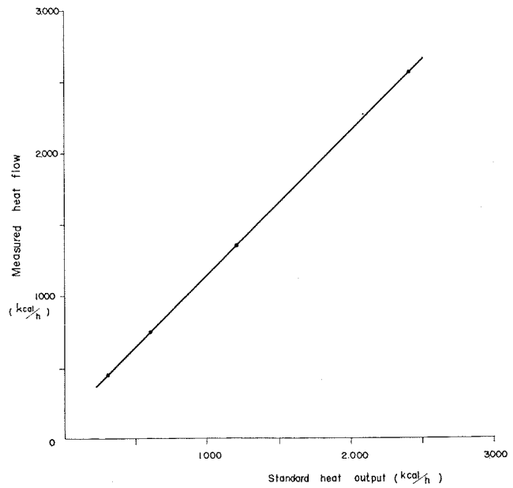

FIG. 4. — *Calibration curve for calorimeter.*

THERMAL DISCHARGE BY GAS

The thermal discharge by gas is given by

$$Q = q \cdot C_p \cdot t / A$$

where

Q is the amount of thermal discharge. q the amount of gas, C_p the specific heat at a constant pressure of gas, t the temperature of the gas, A the area of the vessels' bottom.

The amount of gas flow was about 0.04 Nm^3/m^2 h at the Otake geothermal area and as this value had little effect on the estimation of the total thermal discharge, the thermal discharge by gas was negligible.

Results and concluding remarks

The results of the measurements made at the Otake, Komatsu and Kawara thermal areas are summarized in Table 1.

A comparison of the total thermal discharge of the Otake geothermal area with the others is given in Table 2. The total thermal discharge of the Otake geothermal area seems to be greatly under-estimated since the areas of thermal discharge are limited to those near the fumaroles.

TABLE 1. — *Estimates of the natural heat output of three thermal areas.*

Item	Kawara	Otake	Komatsu	Sujiyu Kijenyu	Total
Total output ($\times 10^4$ kcal/h)	516	559	1185	252	2512
Source of heat (percentage)					
Steam	42.2	50.4	28.5		33.4
Hot water	52.0	20.8	53.5	100	50.4
Conduction	5.8	28.8	18.0		16.2

A comparison of the heat output of five productive wells which were drilled near the Otake fumaroles with the total thermal discharge of the Otake geothermal area is shown in Figure 6.

Measurement of temperature gradient

GENERAL

The geothermal gradient, in general, differs from place to place. In other words, it is different depending on the type of rocks, the existence of underground water

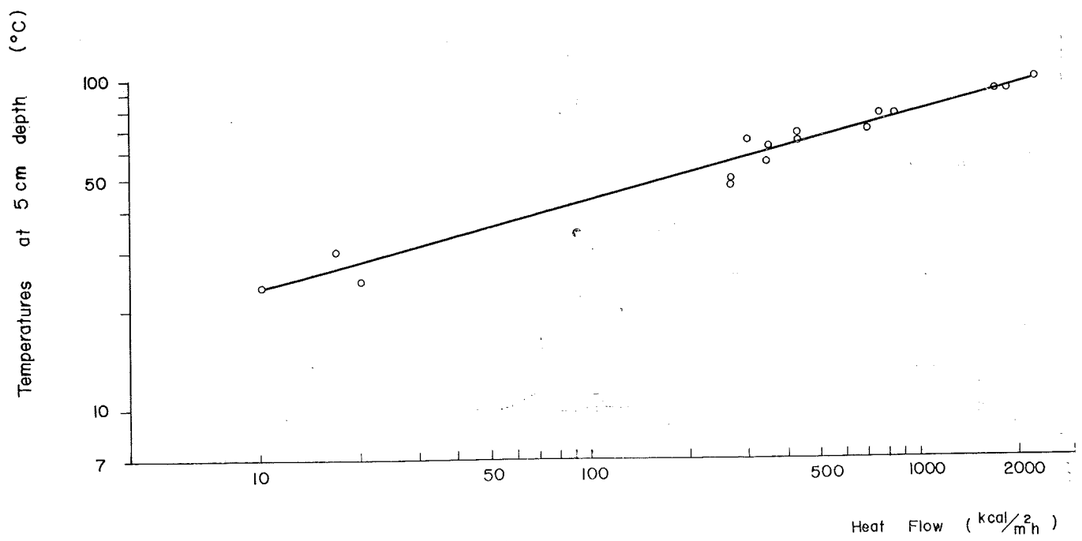

FIG. 5. — *Relation between heat flow and temperatures at 5 cm depth.*

TABLE 2. — *The total natural heat discharge of thermal areas.*

	Natural heat output (1)		Remarks
Atsanupri	28.1		basic temperature 10 °C by T. FUKUDOMI
Noboribetsu	40.6		
Oakudani	38.1		basic temperature 0 °C
Souzan	(33.5)		basic temperature 10 °C
Kawara	5.2		
Otake	5.6	22.6	basic temperature 0 °C
Komatsu	11.8		
Beppu	68.5		—
Atami	57.5		—
Geyser	1.5		by MCNITT 1963
Wairakei	587		by THOMPSON 1959
Larderello	18		thermal discharge by hot springs

(1) $\times 10^6$ kcal/h

and so on. Therefore it is necessary to determine the peculiar value of the local geothermal gradient.

For the purpose of determining the geothermal gradient, two drilling locations were selected in the areas of Komatsu and Otake, shown in Figure 1. A survey hole was drilled in each area. The depth of these holes is 25 m, the diameter 8.5 cm.

METHOD OF TEMPERATURE MEASUREMENT

In order to measure the temperature of fluid in the borehole, a weighted copper-constantan thermocouple lead was lowered along the center of the borehole. This lead has twelve hot junctions at 2 m intervals along the bore, of which the top coincides with 2 m from the ground surface and the bottom is at 24 m. The cold junctions are kept at 0°C in an icejar set at the ground surface.

The temperature of the fluid in the borehole was recorded, for about 120 hours after the circulation of the drilling fluid was stopped, by an automatic electronic-type potentiometer (12 components, maximum sensivity is 15 mV/full scale and chart speed is changeable) manufactured by Yokokawa Electric Co. Ltd.

From that time on, cement milk was poured into the borehole and the copper-constantan thermocouples were fixed. A month later, the temperature of concrete in the borehole was measured.

The recorded temperatures are accurate to $\pm$ 0.5 °C, since the probable error would be no greater than 0.02 mV.

RESULTS OF MEASUREMENT

The numerical values of temperature read from the charts are tabulated in Tables 3 and 4. The plots of these data are shown in Figures 10 and 11, together with the geological section of drilling log on the left hand side and with the relation between the depth and the reciprocal gradient (or geothermic step) on the right

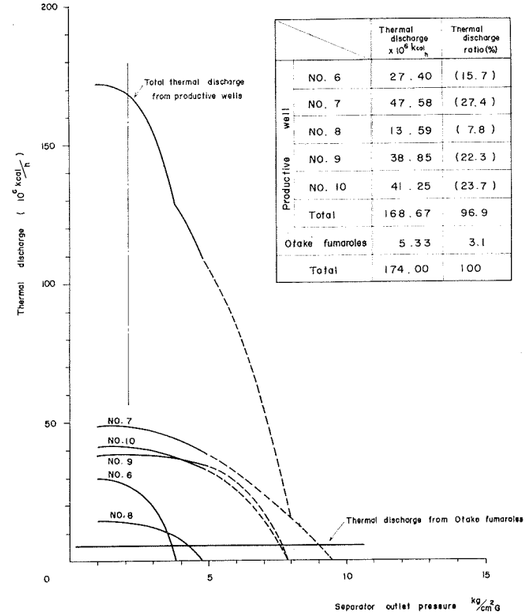

		Thermal discharge $\times 10^6$ kcal/h	Thermal discharge ratio (%)
Productive well	NO. 6	27.40	(15.7)
	NO. 7	47.58	(27.4)
	NO. 8	13.59	(7.8)
	NO. 9	38.85	(22.3)
	NO. 10	41.25	(23.7)
	Total	168.67	96.9
Otake fumaroles		5.33	3.1
Total		174.00	100

FIG. 6. — *Thermal discharge curve.*

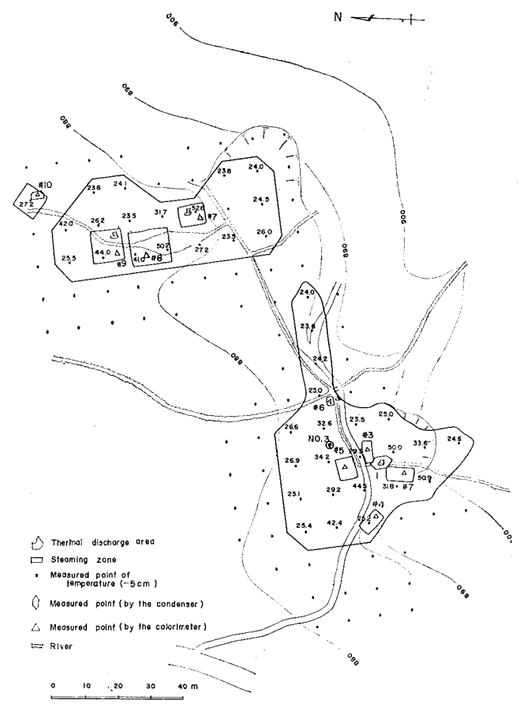

FIG. 7. — *Kawara fumaroles.*

TABLE 3. — *Temperatures in the borehole at the Komatsu area.*

	Mud Water														Concrete
Time (1) (hour)	0.25	0.45	3	4	5	10	15	20	30	40	50	65	85	118	
Depth m	Temperature °C														
2	19.2	18.5	21.5	21.3	**20.5**	20.0	19.0	19.0	18.5	—	19.0	18.8	18.8	18.0	17.2
4	15.8	19.0	21.8	20.0	19.0	17.1	16.6	16.6	15.3	15.1	15.3	15.3	14.8	14.8	12.3
6	16.3	19.0	20.5	20.5	18.5	16.6	15.3	15.6	15.1	14.7	14.8	14.8	14.6	14.6	14.5
8	18.0	18.8	18.5	19.2	18.8	17.1	15.8	16.3	16.0	15.3	15.8	15.6	15.3	15.3	13.2
10	18.8	18.0	19.0	19.2	**19.0**	18.0	17.3	17.3	17.3	16.6	17.3	17.3	17.3	16.9	17.2
12	17.0	18.0	18.5	19.5	18.5	18.8	18.3	18.3	18.5	17.1	18.5	18.5	18.3	18.0	17.4
14	17.6	17.8	19.0	19.8	**19.8**	19.8	19.0	19.0	19.5	19.5	19.8	20.0	19.8	19.5	18.3
16	17.6	18.3	20.5	21.3	**21.0**	21.3	20.0	21.0	20.5	20.5	21.3	21.5	20.7	21.0	21.8
18	17.6	19.5	21.0	22.3	**22.0**	22.7	22.5	22.5	23.0	22.0	23.0	23.0	23.0	23.2	22.3
20	17.6	20.0	22.0	22.5	**22.5**	23.5	23.5	23.2	23.8	23.2	24.0	24.3	24.0	23.8	23.0
22	16.6	20.5	23.0	24.0	24.5	25.0	25.6	25.3	25.8	25.3	26.7	26.7	26.7	26.7	27.3
24	21.3	21.8	24.5	25.0	25.6	27.0	27.2	27.5	27.7	27.5	28.2	28.7	28.2	28.2	28.5

(1) Time is the lapse of time after the circulation of drilling fluid was stopped. The temperature of mud water was measured between 31st August and 5th September and cement milk was poured into the borehole on 5th Sept. 1968. The temperature of the concrete was measured again on 5th October.

TABLE 4. — *Temperatures in the borehole at the Otake area.*

	Mud Water												Concrete
Time (1) (hour)	18	23	28	33	43	53	63	67	89	93	103	112	
Depth m	Temperature °C												
2	59.8	60.3	62.3	63.8	65.0	64.5	64.0	64.5	65.0	65.5	65.8	66.5	98.0
4	73.5	74.8	70.3	76.0	79.0	81.3	82.7	83.7	87.0	86.7	87.5	88.7	100.7
6	78.0	80.5	79.0	82.5	85.0	87.2	90.5	92.0	102.5	102.8	103.3	104.0	103.2
8	91.8	92.7	95.2	95.3	98.0	104.5	104.0	105.0	106.0	105.8	105.8	106.5	101.5
10	97.0	98.5	104.6	102.5	104.5	143.0	104.4	105.5	105.0	103.0	100.7	99.2	106.5
12	96.0	97.7	99.3	100.5	102.5	104.5	105.2	106.3	108.5	108.5	108.5	109.5	111.2
14	95.0	97.0	98.0	98.8	101.0	102.0	103.0	104.0	106.0	106.0	106.7	107.3	108.0
16	100.5	102.5	104.0	104.8	106.5	107.3	108.5	110.0	111.0	111.0	111.3	111.7	112.0
18	108.0	109.5	110.7	111.2	112.7	113.2	113.3	**114.5**	115.7	115.5	115.7	116.0	115.5
20	110.0	111.2	112.0	112.7	114.3	115.0	115.5	116.5	117.5	117.7	117.7	118.3	118.7
22	113.2	114.7	116.3	117.0	118.3	119.5	**120.0**	121.0	122.0	122.3	122.3	122.8	123.2
24	**121.5**	123.0	123.8	124.3	125.0	125.0	125.8	127.0	127.5	127.5	127.3	127.3	127.5

(1) Time is the lapse of time after the circulation of drilling fluid was stopped. The temperature of mud water was measured between 27th and 31st August, 1968. We poured cement milk into the borehole on 31st August and measured the temperature of concrete in the hole on 6th October, 1968.

hand side of each Figure. The result of investigations in the two areas is described briefly as follows.

Komatsu area. Referring to Figure 10, the temperature logs show irregular change at nearly 4 m deep in the borehole. This indication corresponds to the boundary between air and mud water in the borehole. In fact, the level of mud water was at the depth of 4.4 m from the ground surface and the atmospheric temperature was 22.3°C at that time. Apart from this point, the temperature logs marked by 15 min, 45 min, 3 hr, 5 hr, etc., are macroscopically divided into three parts: the first part corresponds to the depth from 6 to 12 m, the second part nearly 14 m deep and the third part to the depth of 16 to 24 m.

In the first part, the temperature of the fluid in the bore gradually drops as time passes. It is evident that the heat flows from the fluid in the bore to the surrounding formation.

The second part shows that the temperature hardly changes after the lapse of three hours under the conditions of the present temperature measurement. In the present study, the location where the temperature hardly changes even if time passes is called a thermal equilibrium point. This point appears at the location where the inlet temperature of the circulating fluid is similar to the temperature of the virgin strata. Such a point can be detected quickly from a few temperature logs, and is useful in determining the geothermal gradient accurately because the temperature at this point hardly varies as time passes.

In the third part, the 15 min curve shows comparatively uniform temperature at the depth of 14 to 20 m, while the temperature at the depth of 24 m quickly

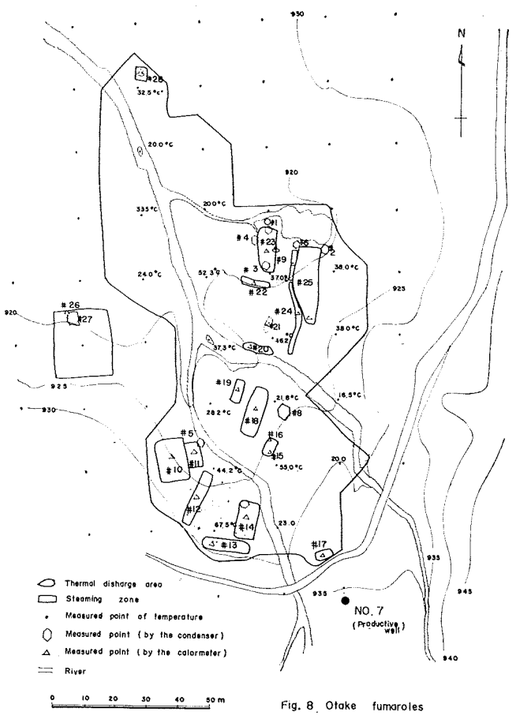

Fig. 8 Otake fumaroles

FIG. 8. — *Otake fumaroles.*

increases. The former is caused by the disturbance of mud water due to the extraction of the drill rod and the latter by the heat generated by the bit action. In general, the temperature in the third part gradually returns to the temperature of the virgin strata with the passing of time.

In the geological field, the geothermic step (or geothermic degree) is frequently used to show the dimension of thermal conductivity. Strictly, the geothermic step is defined by the vertical distance between two points having a temperature difference of one degree. The relation between the geothermic step and depth is shown on the right hand side af Figure 10. Practically, the thermal conductivity corresponding to the bed at the depth of 10 m is greater than that of 18 m. This shows that the thermal conductivity increases with the compactness of rocks.

The depth where the geothermic step changes from negative to positive or vice versa corresponds to a formation boundary. It is therefore expected that such an indication of the geothermic step will enable us to detect the formation boundary from the temperature log.

Otake area

The thermal equilibrium point mentioned above does not appear, since the temperature of the virgin strata along the full length of the borehole is much greater than that of the circulating fluid.

The temperature curves rise gradually as time passes, except the curve marked by 112 h, where the temperature decreases at the depth of 10 m, compared with other curves (Figure 11). It is known from the indication mentioned above that the motion of hot water or the phase change from hot water to vapor takes place at the interface of the strata. Comparing the thermal conductivity at the depth of 10 m with that at the depth of 24 m, the numerical values are of the same order, since the thermal conductivity increases with compactness and decreases as temperature rises, and these two phenomena cancel each other.

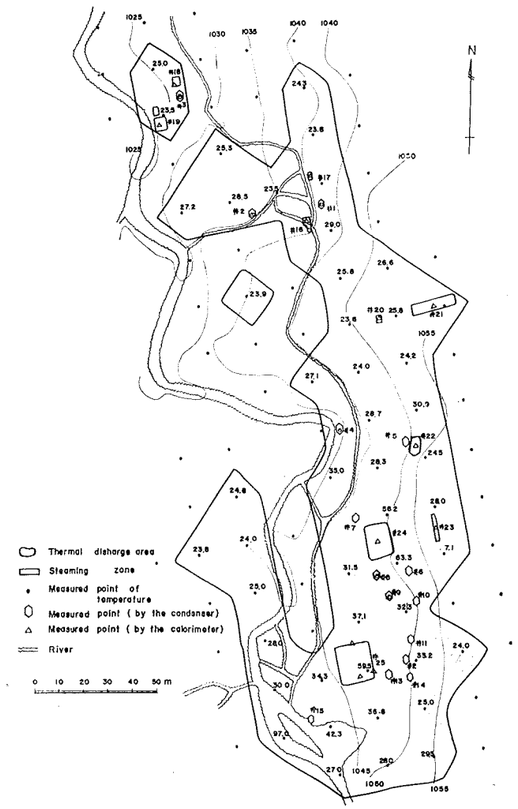

FIG. 9. — *Komatsu fumaroles.*

DISCUSSION ON THE TEMPERATURE LOGGING

The result of numerical calculations of GUYOD's formula is given by the temperature recovery curves with various values of C as shown in Figure 12.

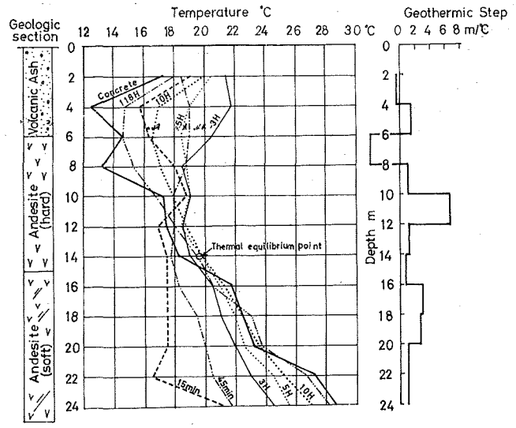

FIG. 10. — *Temperature log at the Komatsu area.*

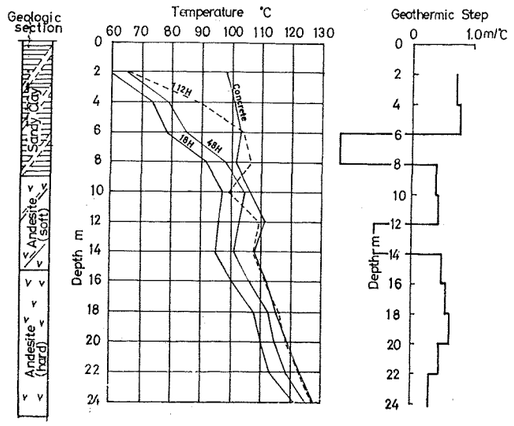

FIG. 11. — *Temperature log at the Otake area.*

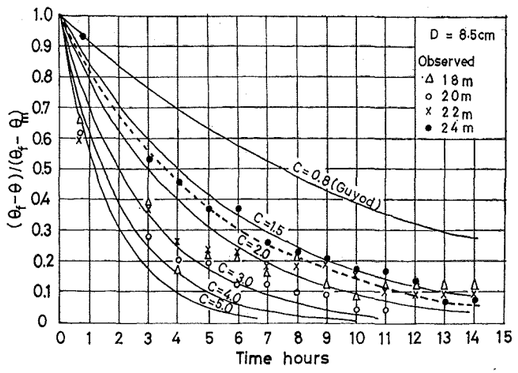

FIG. 12. — *Temperature recovery curves at the Komatsu area.*

Although the fluid temperature may be expected to approach its final value asymptotically, the values of observed temperatures do not lie on the theoretical curves of Guyod because of the temperature disturbance of the surrounding formation caused by circulating fluid, the convection of the fluid in the borehole, the heat from the base of the hole and so on.

Considering the heat from the base of the hole, GUYOD's formula can be improved as follows:

$$\frac{\theta_f - \theta}{\theta_f - \theta_m} = e^{-\frac{4\alpha}{\varrho c}\left(\frac{1}{D}+\frac{1}{4h}\right)t}$$

where

θ_f is the true formation temperature,
θ_m the temperature observed at time $t = 0$,
θ the observed temperature at time t,
α the coefficient of heat transfer between the mud water and the wall of the borehole,
ϱ the fluid density,
c the specific heat of the fluid,
D the diameter of the borehole,
h the length of the borehole to be dealt with,
t the time.

For instance, the length h is the height affected by the heat from the base of the hole.

In Figure 12, the continuous lines show the theoretical curves computed by GUYOD's formula with various values of C and the dotted line shows the one computed by the improved formula, where $C=4\alpha/\varrho c=1.5$ and $h=30$ cm were adopted in the present case.

CONCLUDING REMARKS

1) - From the temperature log obtained, the geothermal gradient was determined as follows: 0.83 °C/m at the Komatsu area where there is no sign of geothermal energy at the ground surface, 1.9 °C/m at the Otake area where fumaroles, hot springs and five productive wells exist.

2) - The thermal equilibrium point appears at the location where the inlet temperature of the circulating fluid is similar to the true formation temperature. This point can be detected quickly by a few temperature logs, and is useful in determining the reliable temperature since the temperature at this point hardly varies with the passing of time.

3) - Computing the geothermic step at small intervals enables us to detect the formation boundary from the temperature log.

4) - From the data on the temperature logging, it is concluded that the temperature return of the fluid to the true formation temperature does not follow GUYOD's formula and the aspect of return seems to be different from depth to depth.

Considering the heat from the base of the hole, the formula can be improved as follows:

$$(\theta_f - \theta) / (\theta_f - \theta_m) = e^{-\frac{4\alpha}{\varrho c}\left(\frac{1}{D}+\frac{1}{4h}\right)t}$$

Measurement of the thermal conductivities of rock samples.

The thermal conductivity of rock samples was measured using the line source method. In this method, a thin nichrome wire and thermocouple (copper-constantan) were used, as the linear heater and the temperature-sensitive element, respectively. The values of the conductivity measured in the laboratory are sometimes different from those measured in situ because of the differences of water content, porosity, temperature, pressure and so on. By measuring temperature gradient, $\left(\frac{\partial T}{\partial z}\right)$, and conductivity, k, the heat flow by conduction toward the earth's surface is given by

$$Q = k\left(\frac{\partial T}{\partial z}\right) \qquad (1)$$

where the z axis is taken vertically downward.

GENERAL THEORY

As many investigators have measured the thermal conductivity of rock by the same method, the theory is briefly described here.

Assuming that the temperature distribution due to a line heat source in a core is the same as the distribution due to a line heat source of infinite length in an infinite homogeneous medium, then we can apply the equation of the form

$$\theta = \frac{q}{4\pi k}\left\{\ln\frac{4\alpha}{a^2\gamma} + \ln t + \frac{a^2}{4\alpha t} - \frac{1}{2\cdot 2!}\left(\frac{a^2}{4\alpha t}\right)^2 + \cdots\right\} \qquad (2)$$

where

θ = temperature of the heater
q = the amount of heat generation of the heater per unit length per unit time
k = thermal conductivity
t = time
α = thermal diffusivity
a = distance between the heater and the temperature-sensitive element.

If the thermocouple is set on the heater's surface, then the distance (a) is very small and if the time (t) is great enough, then the value ($a/4\alpha t$) becomes negligible. Consequently, the equation (2) can be written as

$$\theta \doteqdot \frac{q}{4\pi k}\ln t + C \qquad (3)$$

which shows that a plot of (θ) against (t) is a straight sloping line of slope ($q/4\pi k$), in which the value of (q) is computed from the current (I) and the resistance (R) of the heater.

MEASURING METHOD

Figure 13 shows the measuring system. A small hole, 3.2 mm in diameter, was drilled with a concrete drill along the longitudinal axis of the cylindrical core. The linear heater with a resistance of 0.2491 Ω/cm, 200 mm in length, was inserted in the hole and the thermocouple was placed half way along the heater. Both of them were sheathed with MgO and each outside diameter was 1.0 mm. They were cemented with Wood's metal to eliminate contact resistance of the heater and the thermocouple to the sample. The samples were heated in an oven for an hour to make insertion of the metal easier and cooled to room temperature before measurements were made. The temperature rise versus time was recorded by a one-pen type recorder. The conductivity of the soil was also measured with a potentiometer in situ. Two 6 V batteries were used for the heater (Figure 15).

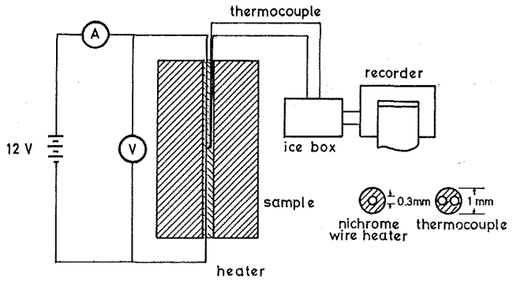

FIG. 13. — *The measuring system of core conductivity.*

SAMPLE

Core samples, 58 mm in diameter, were selected from bore cores of T-2 hole which was bored 1000 m deep near the Komatsu fumaroles several years ago. They were cut with a diamond saw to more than 100 mm in length because they needed to have a length at least 30 times the diameter of the hole. In selecting samples, ones with cracks and those very much altered were omitted, since small holes had to be drilled.

EXPERIMENTAL RESULTS

The values of conductivity are tabulated in Table 5a and the relation between conductivity and depth is plotted in Figure 14. As seen in Figure 14, the tendency is that the greater the depth, the higher the values. The weighted mean value of conductivities computed by

$$\bar{k} = \frac{\Sigma L_i}{\sum \frac{L_i}{k_i}}$$

where

$\bar{k}$ = the weighted mean value
k_i = the thermal conductivity of the ith layer
L_i = thickness of the ith layer.

is 5.24×10^{-3} cal/cm °C sec.

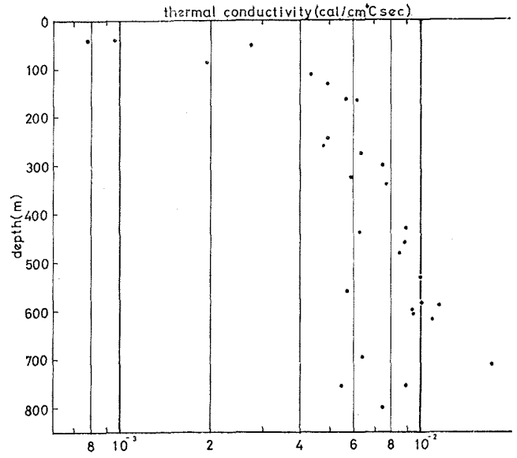

FIG. 14. — *The relation between conductivity and depth.*

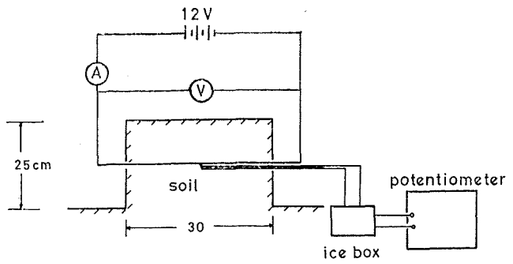

FIG. 15. — *The measuring system of soil conductivity.*

TABLE 5 a. — *Thermal conductivities of rock samples.*

Depth m	Conductivity cal/cm °C sec	Depth m	Conductivity cal/cm °C sec
40	9.52×10^{-4}	439	6.29×10^{-3}
41	7.73×10^{-4}	460	8.80×10^{-3}
51	2.73×10^{-3}	481	8.43×10^{-3}
86	1.93×10^{-3}	532	9.95×10^{-3}
113	4.31×10^{-3}	559	5.70×10^{-3}
131	4.91×10^{-3}	584	1.00×10^{-2}
163	5.63×10^{-3}	588	1.14×10^{-2}
166	6.15×10^{-3}	598	9.32×10^{-3}
244	4.92×10^{-3}	606	$9.38\times10\times^{3}$
260	4.77×10^{-3}	618	1.08×10^{-2}
276	6.31×10^{-3}	699.5	6.44×10^{-3}
300	7.41×10^{-3}	710	1.72×10^{-2}
326	5.88×10^{-3}	752.5	8.91×10^{-3}
340	7.63×10^{-3}	753	5.43×10^{-3}
431	8.90×10^{-3}	799	7.47×10^{-3}

From the weighted mean value of conductivities and the mean temperature gradient from —20 to —300 m of *T*-2, the heat flow

$$Q = 7.7\times10^{-6}\ \text{cal/cm}^2\ \text{sec}$$

is obtained. Table 5b shows the conductivities of the soils, temperature gradients of —25 ∿ —45 cm measured with c-c thermocouple and the computed heat flow. These values of the heat flow are much smaller than those of the thermal discharge measured above but much higher than 1.5×10^{-6} cal/cm² sec of the normal area. For good conducting rocks, the diameter of the core, 58 mm, might not be satisfactory, compared with that of the hole, 3.2 mm, to make measurements for a long time for fear of heat radiation from the core's surface, but it was hard to drill long holes of small diameter with the concrete drill. Soft samples were coated with a binding agent to protect them from breaking while holes were drilled. Because the samples were heated, the water content may be quite small. For hard rocks, the influence of porosity and water content does not have to be considered.

TABLE 5 b. — *Thermal conductivities of the soils and computed heat flow.*

	No.	Conductivity cal/cm °C sec	Temperature gradient °C/cm	Heat flow kcal/m²h
Komatsu	1	2.15×10^{-3}	0.93	60.7
	2	2.67×10^{-3}	1.02	97.9
	3	2.37×10^{-3}	0.89	76.3
Otake	1	2.81×10^{-3}	0.29	29.5
	2	1.99×10^{-3}	0.83	58.4
	3	3.43×10^{-3}	0.39	47.6
	4	2.24×10^{-3}	0.27	22.1

Acknowledgements

We would like to thank Dr. T. NOGUCHI, Dr. S. ONODERA and Dr. T. YAMASAKI, Kyushu University, for their many constructive suggestions. We also thank T. KAI, Kyushu Univ., T. MATSUMOTO, K. IGAWA and other colleagues for their great help.

REFERENCES

GUYOD H. 1946 — Temperature well logging. *Oil Weekly, Oct. 2, Nov. 4, Dec. 2, 9 and 16.*

JAEGER J. C. 1961 — The effect of the drilling fluid on temperatures measured in bore holes. *J. geophys Res.*, 66.

JAEGER J. C. 1965 — Application of the theory of heat conduction to geothermal measurements. *in:* « *Terrestrial Heat Flow* », *Amer. geophys. Un., Geophys. Mon. Ser.*, 8.

LACHENBRUCH A. H. 1957 — A probe for measurement of thermal conductivity of frozen soils in place. *Trans. amer. geophys. Un.*, 38, *991.*